" Synthesis and characterization of novel niccolite metal formate frameworks $[(CH_3)_2NH_2][Fe^{III}M^{II}(HCOO)_6]$ (M^{II}=Zn, Ni, Cu)"

by Aneta Ciupa et al.

Table S1. Data collection, cell, and refinement parameters for DMFeNi.

Crystal data	
Chemical formula	$C_8H_{14}FeNNiO_{12}$
M_r	430.76
Crystal system, space group	Trigonal, $P\bar{3}1c$
Temperature (K)	298
a, c (Å)	8.1856 (7), 13.6517 (17)
V (Å^3)	792.17 (17)
Z	2
Radiation type	Mo $K\alpha$
μ (mm^{-1})	2.16
Crystal size (mm)	0.15 × 0.05 × 0.04

Data collection	
Diffractometer	Xcalibur, Sapphire1, long nozzle diffractometer
Absorption correction	Multi-scan *CrysAlis PRO*, Oxford Diffraction Ltd., Version 1.171.34.44 (release 25-10-2010 CrysAlis171 .NET) (compiled Oct 25 2010,18:11:34) Empirical absorption correction using spherical harmonics, implemented in SCALE3 ABSPACK scaling algorithm.
T_{min}, T_{max}	0.933, 1.000
No. of measured, independent and	5333, 507, 391

observed [$I > 2\sigma(I)$] reflections	
R_{int}	0.078
$(\sin \theta/\lambda)_{max}$ (Å^{-1})	0.608

Refinement	
$R[F^2 > 2\sigma(F^2)]$, $wR(F^2)$, S	0.041, 0.080, 1.10
No. of reflections	507
No. of parameters	42
No. of restraints	14
H-atom treatment	H-atom parameters constrained
$\Delta\rangle_{max}$, $\Delta\rangle_{min}$ (e Å^{-3})	0.42, -0.42

Table S2. Geometric parameters (Å, º) for DMFeNi.

Fe1—O1^{i}	2.029 (3)	Fe2—O2^{viii}	2.023 (3)
Fe1—O1^{ii}	2.029 (3)	Fe2—O2^{ix}	2.023 (3)
Fe1—O1^{iii}	2.029 (3)	Fe2—O2^{x}	2.023 (3)
Fe1—O1^{iv}	2.029 (3)	Fe2—O2	2.023 (3)
Fe1—O1^{v}	2.029 (3)	O1—C1	1.231 (5)
Fe1—O1	2.029 (3)	O2—C1	1.244 (5)
Fe2—O2^{vi}	2.023 (3)	C2—N1	1.444 (10)
Fe2—O2^{vii}	2.023 (3)	C21—N1	1.436 (10)

O1^{i}—Fe1—O1^{ii}	92.87 (12)	O2^{vii}—Fe2—O2^{viii}	88.53 (12)
O1^{i}—Fe1—O1^{iii}	85.06 (17)	O2^{vi}—Fe2—O2^{ix}	91.47 (12)
O1^{ii}—Fe1—O1^{iii}	177.09 (18)	O2^{vii}—Fe2—O2^{ix}	88.53 (12)
O1^{i}—Fe1—O1^{iv}	177.09 (18)	O2^{viii}—Fe2—O2^{ix}	91.47 (12)
O1^{ii}—Fe1—O1^{iv}	89.27 (18)	O2^{vi}—Fe2—O2^{x}	88.53 (12)

O1^{iii}—Fe1—O1^{iv}	92.87 (12)	O2^{vii}—Fe2—O2^{x}	91.47 (12)
O1^{i}—Fe1—O1^{v}	92.87 (12)	O2^{viii}—Fe2—O2^{x}	180.0
O1^{ii}—Fe1—O1^{v}	92.87 (12)	O2^{ix}—Fe2—O2^{x}	88.53 (12)
O1^{iii}—Fe1—O1^{v}	89.27 (18)	O2^{vi}—Fe2—O2	88.52 (12)
O1^{iv}—Fe1—O1^{v}	85.06 (17)	O2^{vii}—Fe2—O2	91.48 (12)
O1^{i}—Fe1—O1	89.27 (18)	O2^{viii}—Fe2—O2	88.52 (12)
O1^{ii}—Fe1—O1	85.06 (17)	O2^{ix}—Fe2—O2	180.0
O1^{iii}—Fe1—O1	92.87 (12)	O2^{x}—Fe2—O2	91.48 (12)
O1^{iv}—Fe1—O1	92.87 (12)	C1—O1—Fe1	126.9 (3)
O1^{v}—Fe1—O1	177.09 (18)	C1—O2—Fe2	125.9 (3)
O2^{vi}—Fe2—O2^{vii}	180.00 (14)	O1—C1—O2	125.5 (4)
O2^{vi}—Fe2—O2^{viii}	91.47 (12)	C21—N1—C2	122 (2)

Symmetry codes: (i) -*y*+1, -*x*+1, -*z*+1/2; (ii) *x*, *x*-*y*+1, -*z*+1/2; (iii) -*x*+*y*, -*x*+1, *z*; (iv) -*y*+1, *x*-*y*+1, *z*; (v) -*x*+*y*, *y*, -*z*+1/2; (vi) *y*-1, -*x*+*y*, -*z*; (vii) -*y*+1, *x*-*y*+2, *z*; (viii) *x*-*y*+1, *x*+1, -*z*; (ix) -*x*, -*y*+2, -*z*; (x) -*x*+*y*-1, -*x*+1, *z*.

Table S3. Hydrogen-bond geometry (Å, º) for DMFeNi.

D—H···*A*	*D*—H	H···*A*	*D*···*A*	*D*—H···*A*
N1—H1*A*···O1^{xi}	0.98	2.41	3.25 (3)	143.7
N1—H1*A*···O1^{xii}	0.98	2.45	3.23 (3)	136.1
N1—H1*B*···O1^{xiii}	0.93	2.18	3.01 (3)	148.9
C2—H2*C*···O2^{xiv}	0.96	2.53	3.385 (5)	148

Symmetry codes: (xi) *x*-*y*+1, -*y*+1, *z*+1/2; (xii) *y*, -*x*+*y*, -*z*+1; (xiii) -*x*, -*y*+1, -*z*+1; (xiv) *x*-*y*+1, *x*+1, -*z*+1.

Table S4. Data collection, cell, and refinement parameters for DMFeCu.

Crystal data	
$C_8H_{14}CuFeNO_{12}$	$\beta = 92.975\ (6)°$
$M_r = 435.6$	$V = 1607.8\ (3)\ Å^3$
Monoclinic, $C2/c$	$Z = 4$
$a = 8.3771\ (8)$ Å	radiation, $\lambda = 1.5418$ Å
$b = 14.0950\ (14)$ Å	$T = 293$ K
$c = 13.6352\ (15)$ Å	
Data collection	
$2\theta_{min} = 5.02°,\ 2\theta_{max} = 69.99°,\ 2\theta_{step} = 0.03°$	
Refinement	
$R_p = 0.023$	31 restraints
$R_{wp} = 0.035$	0 constraints
$R_{exp} = 0.010$	H-atom parameters constrained
$R(F) = 0.142$	Weighting scheme based on measured s.u.'s
$\chi^2 = 11.972$	$(\Delta/\sigma)_{max} = 0.044$
2856 data points	Background function: 8 Legendre polynoms
Profile function: Pseudo-Voigt	Preferred orientation correction: March & Dollase
42 parameters	

Table S5. Geometric parameters (Å, º) for DMFeCu.

Cu1—O1	2.08 (3)	Fe—O2	1.90 (3)
Cu1—O1^{i}	2.08 (3)	Fe—O2^{ii}	1.90 (3)
Cu1—O12	2.10 (3)	Fe—O22	2.08 (3)
Cu1—O12^{i}	2.10 (3)	Fe—O22^{ii}	2.08 (3)
Cu1—O13	2.19 (3)	Fe—O23^{iii}	1.94 (3)
Cu1—O13^{i}	2.19 (3)	Fe—O23^{iv}	1.94 (3)

O1—Cu1—O1^{i}	98.8 (13)	O2—Fe—O2^{ii}	180.0 (5)
O1—Cu1—O12	86.9 (11)	O2—Fe—O22	90.0 (13)
O1—Cu1—O12^{i}	172.1 (12)	O2—Fe—O22^{ii}	90.0 (13)
O1—Cu1—O13	95.7 (13)	O2—Fe—O23^{iii}	90.0 (12)
O1—Cu1—O13^{i}	81.3 (12)	O2—Fe—O23^{iv}	90.0 (12)
O1^{i}—Cu1—O12	172.1 (12)	O2^{ii}—Fe—O22	90.0 (13)
O1^{i}—Cu1—O12^{i}	86.9 (11)	O2^{ii}—Fe—O22^{ii}	90.0 (13)
O1^{i}—Cu1—O13	81.3 (12)	O2^{ii}—Fe—O23^{iii}	90.0 (12)
O1^{i}—Cu1—O13^{i}	95.7 (13)	O2^{ii}—Fe—O23^{iv}	90.0 (12)
O12—Cu1—O12^{i}	88.0 (13)	O22—Fe—O22^{ii}	180.0 (5)
O12—Cu1—O13	92.9 (11)	O22—Fe—O23^{iii}	92.5 (12)
O12—Cu1—O13^{i}	90.5 (11)	O22—Fe—O23^{iv}	87.5 (12)
O12^{i}—Cu1—O13	90.5 (11)	O22^{ii}—Fe—O23^{iii}	87.5 (12)
O12^{i}—Cu1—O13^{i}	92.9 (11)	O22^{ii}—Fe—O23^{iv}	92.5 (12)
O13—Cu1—O13^{i}	175.3 (14)	O23^{iii}—Fe—O23^{iv}	180.0 (5)

Symmetry codes: (i) -*x*+1, *y*, -*z*+1/2; (ii) -*x*+1, -*y*+1, -*z*; (iii) -*x*+3/2, *y*-1/2, -*z*+1/2; (iv) *x*-1/2, -*y*+3/2, *z*-1/2.

Table S6. The correlation diagram showing number of expected vibrational modes for DMFeZn and DMFeNi ($P\bar{3}1c$ space group) and DMFeCu ($C2/c$ space group). The data for the C2/c

structure are given in parentheses. Red and black colors correspond to Raman- and IR-active modes, respectively. Blue color denote modes active both in Raman and IR spectra and green corresponds to silent modes.

ion	vibration	Free ion symmetry	Site symmetry	Factor group symmetry
HCOO-		**C_{2v}**	**C_1 (C_1)**	**D_{3d} (C_{2h})**
	ν_1, ν_2 or ν_3	A_1	A (3A)	$A_{1g}+A_{2g}+2E_g+A_{1u}+A_{2u}+2E_u$ ($3A_g+3B_g+3A_u+3B_u$)
	ν_4, ν_5 or ν_6	B_1	A (3A)	$A_{1g}+A_{2g}+2E_g+A_{1u}+A_{2u}+2E_u$ ($3A_g+3B_g+3A_u+3B_u$)
	T’	$A_1 + B_1 + B_2$	3A (9A)	$3A_{1g}+3A_{2g}+6E_g+3A_{1u}+3A_{2u}+6E_u$ ($9A_g+9B_g+9A_u+9B_u$)
	L	$A_2 + B_1 + B_2$	3A (9A)	$3A_{1g}+3A_{2g}+6E_g+3A_{1u}+3A_{2u}+6E_u$ ($9A_g+9B_g+9A_u+9B_u$)
DMA^+		**C_{2v}**	**C_2 (C_2)**	**D_{3d} (C_{2h})**
	$\nu_s(NH_2)$	A_1	A (A)	(A_g+A_u)
	$\nu_{as}(NH_2)$	B_2	B (B)	(B_g+B_u)
	$\delta(NH_2)$	A_1	A (A)	(A_g+A_u)
	$\rho(NH_2)$	B_2	B (B)	(B_g+B_u)
	$\omega(NH_2)$	B_1	B (B)	(B_g+B_u)
	$\tau(NH_2)$	A_2	A (A)	(A_g+A_u)
	$\nu_s(CNC)$	A_1	A (A)	(A_g+A_u)
	$\nu_{as}(CNC)$	B_1	B (B)	(B_g+B_u)
	$\delta(CNC)$	A_1	A (A)	(A_g+A_u)
	$\nu_s(CH_3)$	A_1+B_1	A+B (A+B)	$A_{1g}+A_{2g}+A_{1u}+A_{2u}$ ($A_g+B_g+A_u+B_u$)
	$\nu_{as}(CH_3)$	$A_1+B_1+B_2+A_2$	2A+2B (2A+2B)	$2E_g+2E_u$ ($2A_g+2B_g+2A_u+2B_u$)
	$\delta_s(CH_3)$	A_1+B_1	A+B (A+B)	$A_{1g}+A_{2g}+A_{1u}+A_{2u}$ ($A_g+B_g+A_u+B_u$)
	$\delta_{as}(CH_3)$	$A_1+B_1+B_2+A_2$	2A+2B (2A+2B)	$2E_g+2E_u$ ($2A_g+2B_g+2A_u+2B_u$)

	$\rho(CH_3)$	$A_1+B_1+B_2+A_2$	2A+2B (2A+2B)	$2E_g+2E_u$ ($2A_g+2B_g+2A_u+2B_u$)
	$\tau(CH_3)$	A_2+B_2	A+B (A+B)	$A_{1g}+A_{2g}+A_{1u}+A_{2u}$ ($A_g+B_g+A_u+B_u$)
	T’	$A_1 + B_1 + B_2$	A+2B (A+2B)	($A_g+2B_g+A_u+2B_u$)
	L	$A_2 + B_1 + B_2$	A+2B (A+2B)	($A_g+2B_g+A_u+2B_u$)
M^{2+}/Fe^{3+} (Cu^{2+})			**D_3 (C_2)**	**D_{3d} (C_{2h})**
			A_2 (A)	$A_{2u}+A_{2g}$ (A_g+A_u)
			E (2B)	E_g+E_u ($2B_g+2B_u$)
M^{2+}/Fe^{3+} (Fe^{3+})			**S_6 (C_i)**	**D_{3d} (C_{2h})**
			A_u (A_u)	$A_{1u}+A_{2u}$ (A_u+B_u)
			E_u ($2A_u$)	$2E_u$ ($2A_u+2B_u$)

Table S7. Room-temperature IR and Raman frequencies (in cm^{-1}) of DMFeZn, DMFeNi and DMFeCu and suggested assignments.[a]

DMFeZn	DMFeNi	DMFeCu

Raman	IR	Raman	IR	Raman	IR	Assignment
	3181w		3188w		3187w	$\nu(NH_2)$
	3104w		3103w		3115w	$\nu(NH_2)$
3047m	3145vw	3047m	3044vw	3045w		$\nu_{as}(CH_3)$
3040m	3038vw	3039m	3037vw	3039m	3038vw	$\nu_{as}(CH_3)$
2976s	2974w	2977s	2974w	2974s	2970w	$\nu_s(CH_3)$
	2924w	2903sh			2923w	overtone
2883s	2880m	2886s	2884m	2877m	2874m	$\nu_1(HCOO^-)$
					2838w	$\nu(NH_2)$
					2804m	$\nu(NH_2)$
2830w		2829w		2830w		overtone
					2793w	$2\nu_2(HCOO^-)$
2768w	2770w	2769w	2774w		2765w	$2\nu_2(HCOO^-)$
1678s		1672s		1675s		ν(C-O)
	1596s		1594s		1588s	$\nu_4(HCOO^-)$
1581w	1583s	1583w	1584s	1573w	1568s	$\nu_4(HCOO^-)$
1563w		1560w		1552w		overtone
	1469sh		1472sh			$\delta_{as}(CH_3)$
1463w	1461sh	1464w	1463sh	1468w	1461w	$\delta_s(CH_3)$
	1452w		1452w			$\delta_{as}(CH_3)$
1392s	1385m	1391s	1389m	1388s	1384m	$\nu_5(HCOO^-)$
			1379m			$\nu_5(HCOO^-)$
1370m	1366sh	1366sh	1365m	1374w		$\nu_2(HCOO^-)$
				1352w	1354sh	$\nu_2(HCOO^-)$
1341s	1347s	1331m	1335s	1327m	1326s	$\nu_2(HCOO^-)$
1260vw		1257vw				$\rho(CH_3)$

1238w		1237w		1239vw		$\rho(CH_3)$
1088w	1085w	1088w	1086w	190vw	1087w	$\rho(CH_3)$
1071w	1067w	1070w	1064w	1069w	1065w	$\nu_6(HCOO^-)$
	1030w		1031w		1033w	$\rho(CH_3)$
1019w	1014m	1020w	1016m	1022w	1019m, 1015m	$\nu_{as}(CNC)$
886m	885w	888m	884w	890m	885w	$\nu_s(CNC)$
	853w		852w			$\rho(NH_2)$
819m	816s	823m	822s	826m	822s	$\nu_3(HCOO^-)$
	806sh		815sh	809sh	808s, 803sh	$\nu_3(HCOO^-)$
404m		411m		414m		$\delta(CNC)$
	371m		372m		384sh, 345s	T'(Fe,M)
315w, 288w	286w	308w	310w	300w	306w	$T'(HCOO^-)$
	277sh		280w		286w, 278w	$T'(HCOO^-)$
261w		265w				$T'(HCOO^-)$
241w	233sh	255w	252w	235w	242w	$T'(HCOO^-)$
	204sh		225w		218vw	$T'(HCOO^-)$
196w	175w	212w	193w	190w	191w	$L(HCOO^-)$
				185w		$L(HCOO^-)$
149m		169m		164m		$L(HCOO^-)$
125w	109w	125w	117w	127w	128w, 109w	$L(HCOO^-)$
80w		83w		77w		T'(DMA)

[a]Key: s, strong; m, medium; w, weak; vw, very weak; sh, shoulder; b, broad; ν, stretching; δ, in-plane bending; τ, torsion; ω, wagging; ρ, rocking; T', translation; L, libration

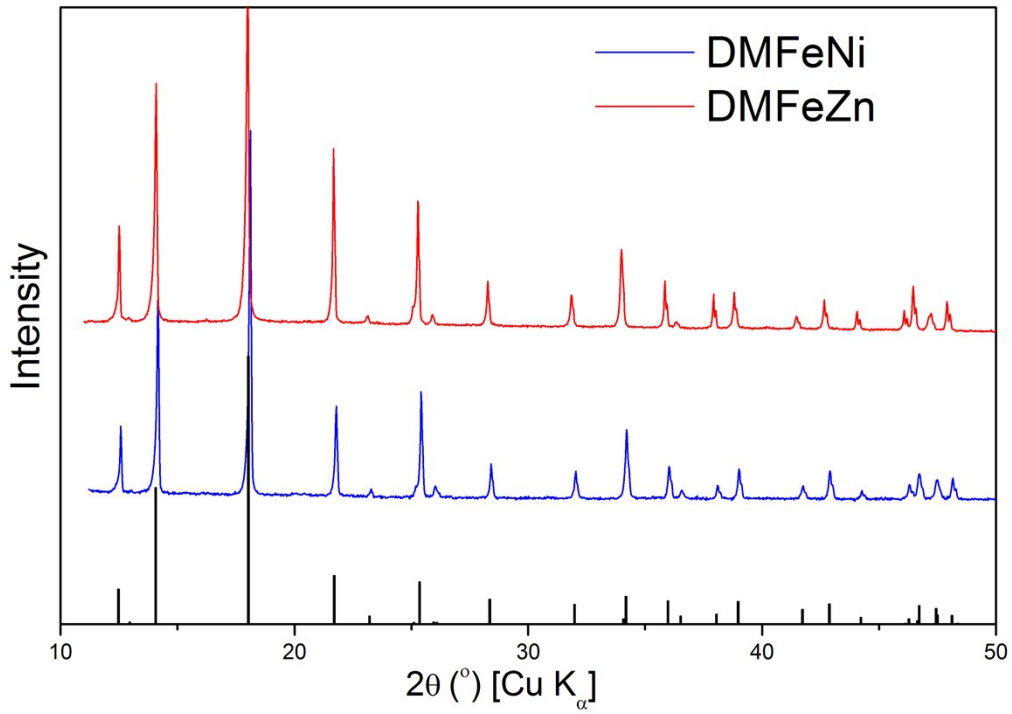

Figure S1. XRD patterns for DMFeNi and DMFeZn. Black bars at the bottom show position and relative intensity of DMFeNi diffraction patterns.

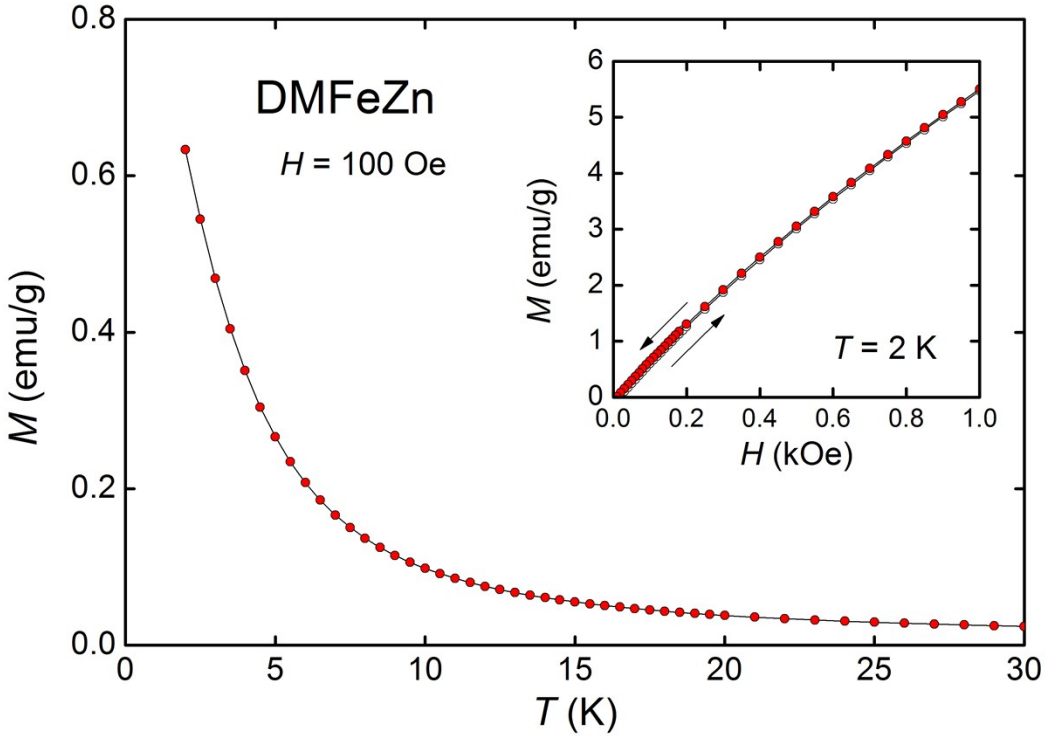

Figure S2. Magnetization of DMFeZn vs. temperature. Inset: *M(H)* measured upon increasing and decreasing field (open and closed symbols, respectively). Solid lines and arrows serve as guides for the eye.

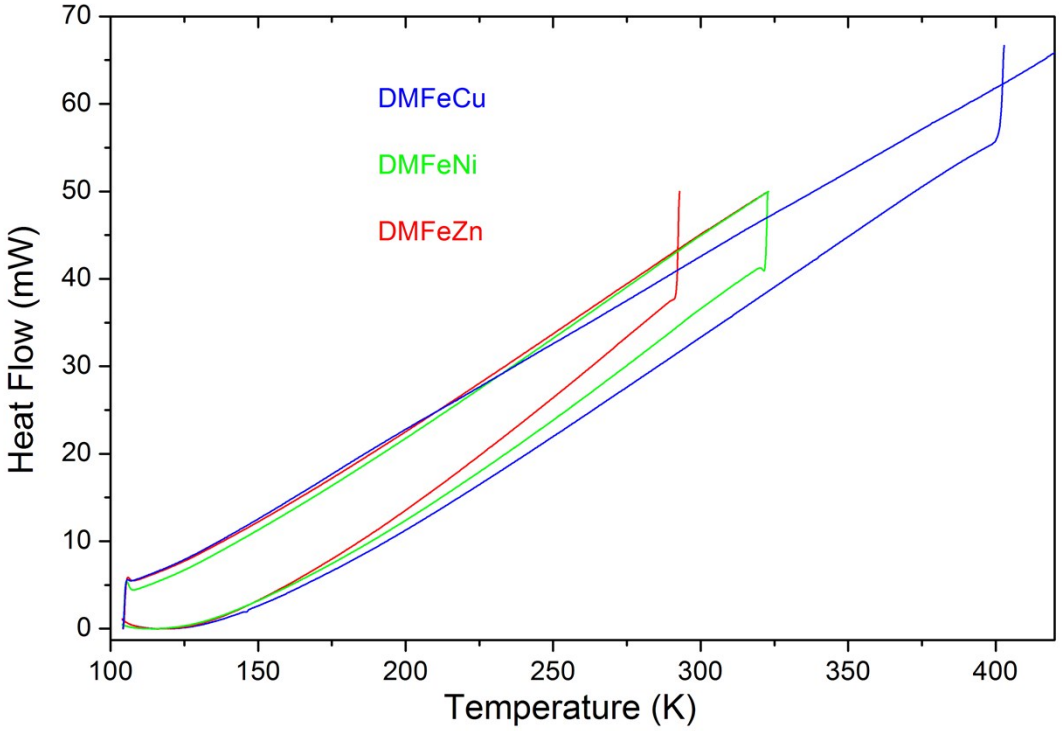

Figure S3. DSC traces for DMFeZn, DMFeNi and DMFeCu.

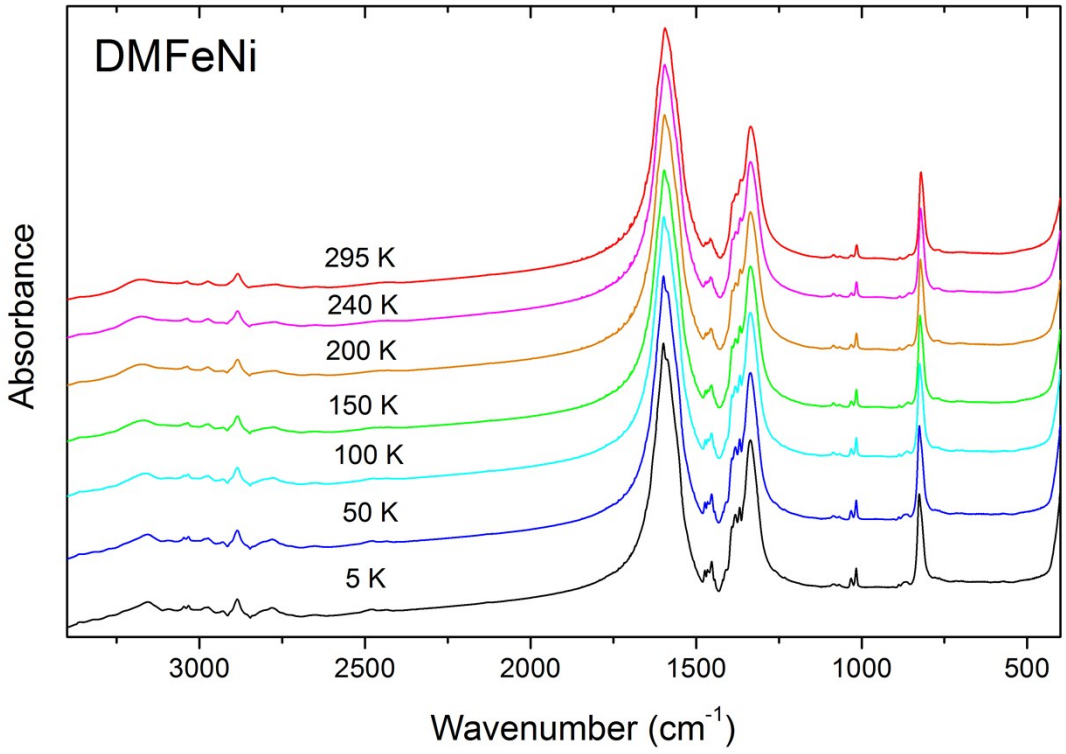

Figure S4. IR spectra of DMFeNi recorded at various temperatures.

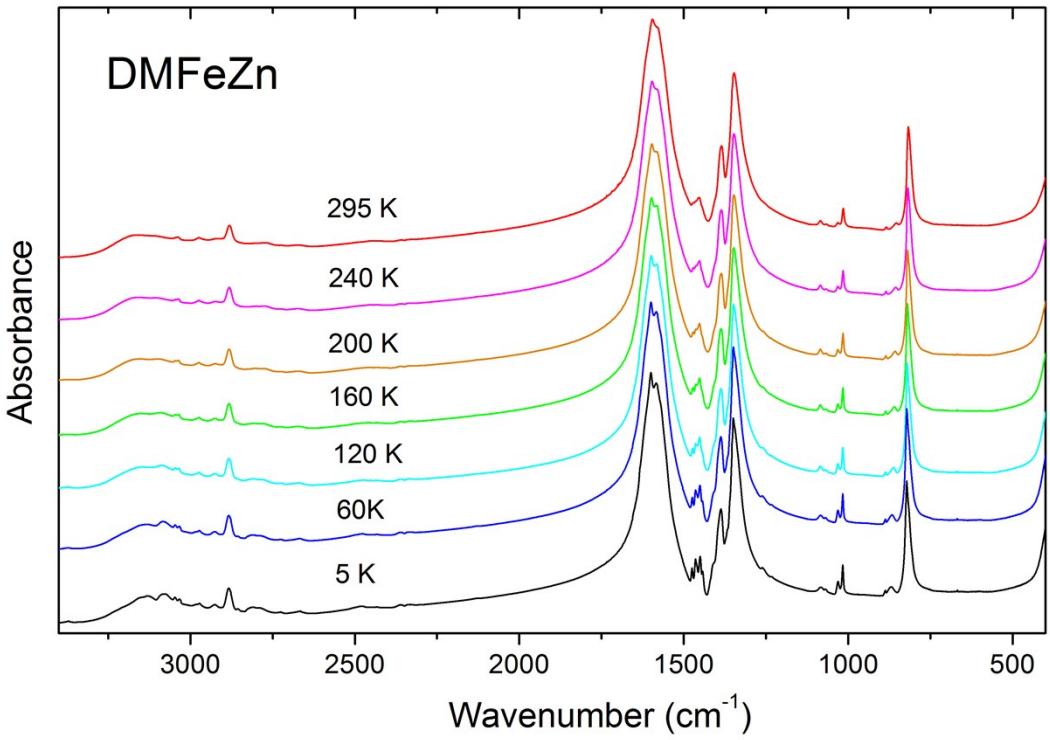

Figure S5. IR spectra of DMFeZn recorded at various temperatures.

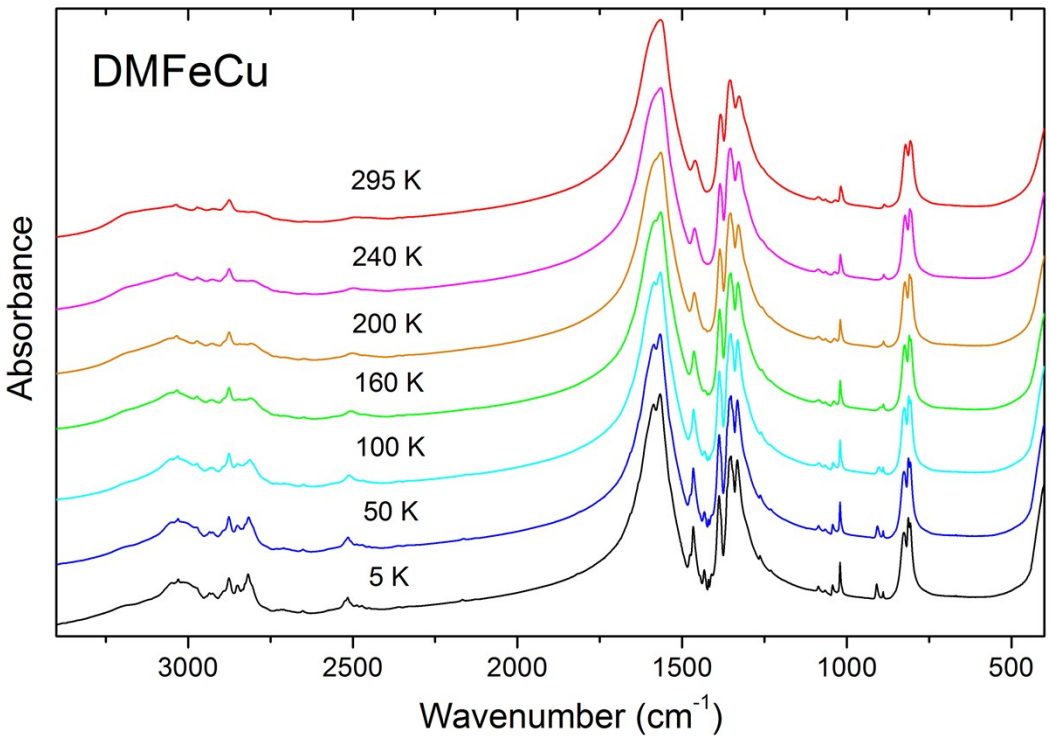

Figure S6. IR spectra of DMFeCu recorded at various temperatures.

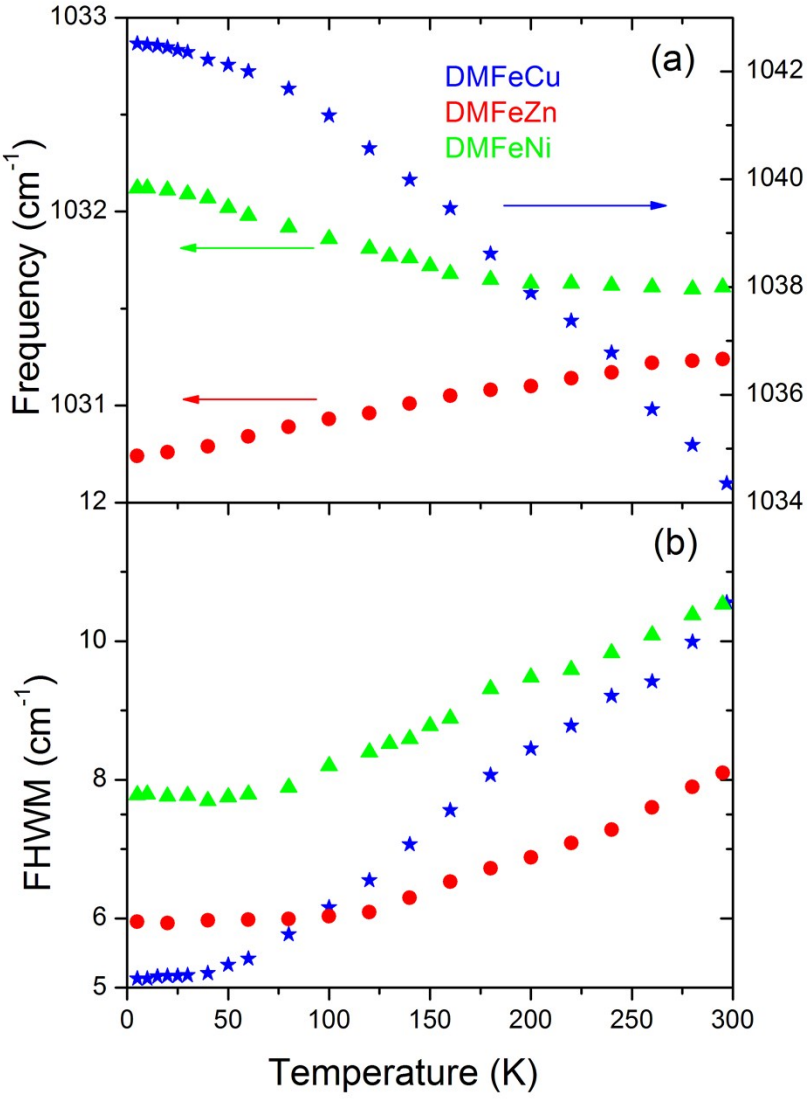

Figure S7. (a) Temperature dependence of the $\rho(CH_3)$ IR frequencies and (b) the corresponding FWHM values for DMFeZn, DMFeNi and DMFeCu. The change of frequency is about 8 times larger for DMFeCu than DMFeZn and DMFeNi. DMFeCu also exhibit more pronounced change in FWHM.

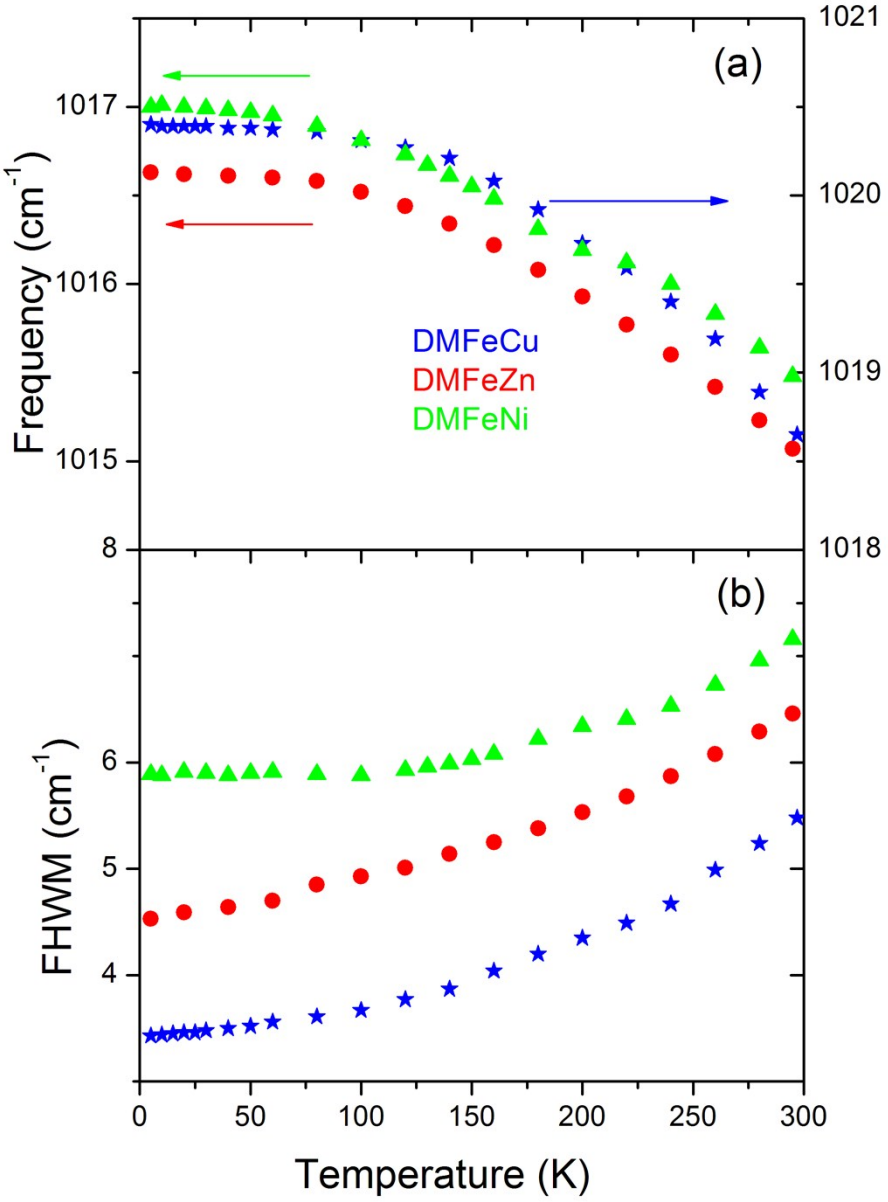

Figure S8. (a) Temperature dependence of the ν_{as}(CNC) IR frequencies and (b) the corresponding FWHM values for DMFeZn, DMFeNi and DMFeCu.